

Wheat Stripe Rust Resistance Protein WKS1 Reduces the Ability of the Thylakoid-Associated Ascorbate Peroxidase to Detoxify Reactive Oxygen Species^{OPEN}

Jin-Ying Gou,^{a,b} Kun Li,^{a,c} Kati Wu,^a Xiaodong Wang,^a Huiqiong Lin,^a Dario Cantu,^d Cristobal Uauy,^{e,f} Albor Dobon-Alonso,^e Takamufi Midorikawa,^a Kentaro Inoue,^a Juan Sánchez,^a Daolin Fu,^c Ann Blechl,^g Emma Wallington,^f Tzion Fahima,^h Madhu Meeta,ⁱ Lynn Epstein,^j and Jorge Dubcovsky^{a,k,1}

^aDepartment of Plant Sciences, University of California, Davis, California 95616

^bState Key Laboratory of Genetic Engineering, Institute of Plant Biology, School of Life Sciences, Fudan University, Shanghai 200433, China

^cState Key Laboratory of Crop Biology, Shandong Agricultural University, Tai'an, Shandong 271018, China

^dDepartment of Viticulture and Enology, University of California, Davis, California 95616

^eJohn Innes Centre, Norwich Research Park, Norwich NR4 7UH, United Kingdom

^fNational Institute of Agricultural Botany, Cambridge CB3 0LE, United Kingdom

^gU.S. Department of Agriculture-Agricultural Research Service, Western Regional Research Center, Albany, California 94710

^hInstitute of Evolution and the Department of Evolutionary and Environmental Biology, University of Haifa, Haifa 31905, Israel

ⁱDepartment of Plant Breeding and Genetics, Punjab Agricultural University, Ludhiana 141004, Punjab, India

^jDepartment of Plant Pathology, University of California, Davis, California 95616

^kHoward Hughes Medical Institute, Chevy Chase, Maryland 20815

ORCID IDs: 0000-0002-9814-1770 (C.U.); 0000-0002-7571-4345 (J.D.)

Stripe rust is a devastating fungal disease of wheat caused by *Puccinia striiformis* f. sp. *tritici* (*Pst*). The *WHEAT KINASE START1* (*WKS1*) resistance gene has an unusual combination of serine/threonine kinase and START lipid binding domains and confers partial resistance to *Pst*. Here, we show that wheat (*Triticum aestivum*) plants transformed with the complete *WKS1* (variant *WKS1.1*) are resistant to *Pst*, whereas those transformed with an alternative splice variant with a truncated START domain (*WKS1.2*) are susceptible. *WKS1.1* and *WKS1.2* preferentially bind to the same lipids (phosphatidic acid and phosphatidylinositol phosphates) but differ in their protein-protein interactions. *WKS1.1* is targeted to the chloroplast where it phosphorylates the thylakoid-associated ascorbate peroxidase (tAPX) and reduces its ability to detoxify peroxides. Increased expression of *WKS1.1* in transgenic wheat accelerates leaf senescence in the absence of *Pst*. Based on these results, we propose that the phosphorylation of tAPX by *WKS1.1* reduces the ability of the cells to detoxify reactive oxygen species and contributes to cell death. This response takes several days longer than typical hypersensitive cell death responses, thus allowing the limited pathogen growth and restricted sporulation that is characteristic of the *WKS1* partial resistance response to *Pst*.

INTRODUCTION

Wheat (*Triticum aestivum* and *Triticum turgidum*) provides roughly 20% of the calories and 25% of the protein consumed worldwide (<http://faostat3.fao.org/>). Although more than 700 million tons of wheat are produced per year, further increases are required to match the demand of a continuously growing human population. One avenue to increase wheat production is to reduce losses caused by wheat pathogens. Among these, *Puccinia striiformis* f. sp. *tritici* (*Pst*), the causal agent of wheat stripe rust (also known as yellow rust), is responsible for major yield losses in most wheat-producing areas. Recent worldwide epidemics are associated with the emergence of new virulent and highly aggressive *Pst* races that are now found at high

frequencies on five continents (Milus et al., 2009; Hovmöller et al., 2010). The most effective and environmentally friendly strategy to limit yield losses caused by *Pst* has been the deployment of resistance genes, which for yellow rust are known as *Yr* genes (McIntosh et al., 2013; Maccaferri et al., 2015).

Wheat rust resistance genes are divided into two general categories: race-specific and race nonspecific (Lowe et al., 2011). Most race-specific resistance genes encode NB-LRR proteins, which include a nucleotide binding (NB) site domain and a leucine-rich repeat (LRR) (Michelmore et al., 2013). These genes, referred to hereafter as *R* genes, detect the presence of specific races of the pathogen and initiate a hypersensitive reaction (Spoel and Dong, 2012). Hypersensitive reactions are characterized by the fast accumulation of reactive oxygen species (ROS) (Torres, 2010) and a rapid programmed cell death of the infected cells, which limits further pathogen colonization of the host (Coll et al., 2011). By contrast, the molecular mechanisms involved in race nonspecific resistance genes are still poorly understood. In the wheat-rust pathosystem, this type of resistance is usually associated with a “slow rusting” or “partial resistance” phenotype because the pathogen is able to

¹ Address correspondence to jdubcovsky@ucdavis.edu.

The author responsible for distribution of materials integral to the findings presented in this article in accordance with the policy described in the Instructions for Authors (www.plantcell.org) is: Jorge Dubcovsky (jdubcovsky@ucdavis.edu).

^{OPEN}Articles can be viewed online without a subscription.

www.plantcell.org/cgi/doi/10.1105/tpc.114.134296

establish itself, but is restricted in its growth and sporulation. Only two race nonspecific resistance genes against the wheat rusts have been identified so far (Fu et al., 2009; Krattinger et al., 2009), and their resistance mechanisms have been unclear.

One of these partial resistance genes is *Yr36*, which was cloned from wild tetraploid wheat (*T. turgidum* ssp. *dicoccoides*) (Fu et al., 2009). *Yr36* encodes a protein designated as WHEAT KINASE START1 (WKS1) that is composed of a serine/threonine kinase domain and a steroidogenic acute regulatory protein-related lipid transfer (START) domain (Fu et al., 2009). The WKS1 kinase present in the N-terminal region is a functional non-arginine-aspartate (non-RD) kinase (Fu et al., 2009). The START domain in the C-terminal region of WKS1 is most similar to the START domain in *Arabidopsis thaliana* ENHANCED DISEASE RESISTANCE2 (EDR2), a protein that negatively regulates plant defense to the powdery mildew pathogen *Golovinomyces cichoracearum* (Tang et al., 2005; Vorwerk et al., 2007). START domains are characterized by a hydrophobic ligand binding pocket and are involved in lipid/sterol binding, transport, and signaling in both animal and plant species (Schrack et al., 2014), but the lipid ligands for the START domains present in WKS1 and EDR2 have not yet been characterized.

Single amino acid substitutions in either the START or the kinase domain result in susceptible phenotypes, indicating that both domains are required for *Pst* resistance (Fu et al., 2009). Two major alternative splice variants of *WKS1* have been detected: *WKS1.1*, which encodes the complete protein, and *WKS1.2*, which encodes a protein with a START domain truncated at the C terminus as a result of the exclusion of exon 11 (Figure 1A). Our previous study has shown that the transcript levels of *WKS1.1* relative to *WKS1.2* increase during the first days of *Pst* infection and at higher temperatures (Fu et al., 2009). In this study, we establish that *WKS1.1* (but not *WKS1.2*) confers resistance to *Pst* in wheat (*T. aestivum*) and advance our understanding of the molecular mechanisms associated with *WKS1.1* partial resistance to *Pst*.

RESULTS

WKS1 Resistance Response against *Pst* Takes Several Days Longer Than Typical Hypersensitive Responses

To understand better the dynamics of the *Pst* infection in the presence and absence of *WKS1*, we characterized pathogen growth and development in the interveinal regions of leaves in three pairs of hexaploid wheat isogenic lines (UC1041 with and without *WKS1* and two pairs of sister lines each with and without a loss-of-function mutation in the *WKS1* kinase domain; Fu et al., 2009). To visualize the fungus, segments of leaves were stained with Uvitex 2B (Polysciences). During the first 6 d post-inoculation (dpi), we detected no significant differences in fungal development between the lines with and without *WKS1* (Supplemental Figure 1). In the second week after inoculation, the susceptible control lines showed a significantly higher percentage of interveinal zones with advanced pathogen networks than the isogenic lines with a functional *WKS1* (10 and 13 dpi; Supplemental Figure 1). The differential resistance response of lines with and without *WKS1* at the different time points resulted

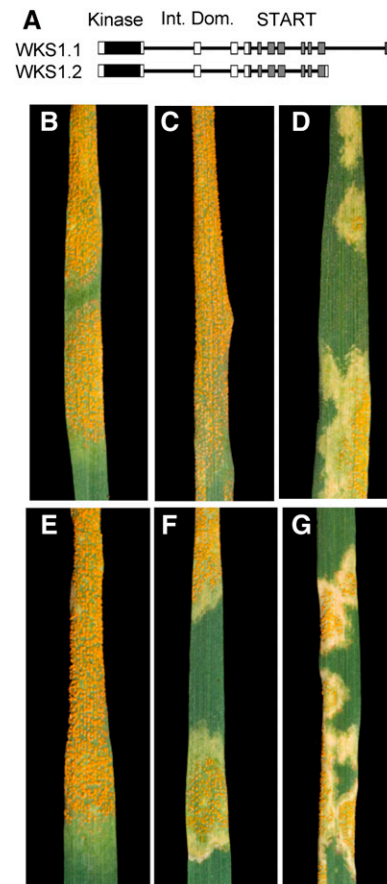


Figure 1. Wheat Plants Transformed with NP:WKS1.1 and NP:WKS1.2 and Inoculated with *Pst* Race PST-08/21.

(A) Schematic representation of *WKS1.1* and *WKS1.2* genes. Introns are represented by black lines and exons by boxes: black = kinase domain, white = inter domain, and gray = START domain.

(B) to (G) Stripe rust infection severity in plants inoculated with PST-08/21 15 dpi.

(B) Susceptible control Glasgow.

(C) Susceptible control UC1041.

(D) Resistant control UC1041+WKS1.

(E) Glasgow transformed with NP:WKS1.2. NP, native promoter.

(F) and (G) Two independent transformation events with NP:WKS1.1.

in a significant interaction between genotype and time after inoculation (two-way factorial ANOVA, $P < 0.0001$). In summary, the progression of *WKS1*-based resistance response to *Pst* described here takes several days longer than typical wheat hypersensitive reaction responses to *Pst* described in previous studies, which show necrotic cells within 2 to 4 dpi (Wang et al., 2007).

Alternative Splice Variant *WKS1.1*, but Not *WKS1.2*, Confers Resistance to *Pst*

To investigate the roles of *WKS1* alternative splice variants (Figure 1A) in *Pst* resistance, we transformed the susceptible hexaploid wheat variety Glasgow with constructs including

WKS1.1 and *WKS1.2* coding regions under the control of the native promoter (Table 1, NP:WKS1.1 and NP:WKS1.2). We then used *Pst* race PST-08/21 (Cantu et al., 2013) to inoculate transgenic plants expressing each alternative splice variant, as well as nontransgenic control plants and isogenic hexaploid wheat lines with and without the wild-type *WKS1* gene (UC1041+*WKS1* and UC1041, respectively) (Fu et al., 2009). All six independent transgenic events carrying NP:WKS1.2 were as susceptible to *Pst* as Glasgow and UC1041 susceptible controls (Figures 1B, 1C, and 1E). By contrast, all five transgenic wheat lines carrying the alternative splice variant NP:WKS1.1 were resistant to PST-08/21 (Figures 1F and 1G) and showed the characteristic partial resistance response observed in the resistant control UC1041+*WKS1* (Figure 1D). For each transgenic event, we calculated the average resistance and \pm SE using 5 to 10 plants per event (Supplemental Table 1). Representative pictures of the *Pst* reactions for each transgenic event are provided in Supplemental Figure 2. To investigate possible causes of the different resistance responses of *WKS1.1* and *WKS1.2*, we analyzed their lipid binding profiles, their ability to form homodimers, and their ability to interact with other proteins.

WKS1.1 and WKS1.2 Have Similar Lipid Binding Profiles

In vitro lipid binding assays were used to assess the ability of full-length proteins *WKS1.1* and *WKS1.2* to bind to membrane lipids and to test if the binding was mediated by the START domain. In the first experiment, we tested 15 different membrane lipids that were immobilized onto a nitrocellulose membrane (Figure 2A). Using polyclonal antibodies raised against glutathione *S*-transferase (GST), we found that both GST-*WKS1.1* and GST-*WKS1.2* proteins (produced by wheat germ in vitro translation) had clear affinities for phosphatidic acid (PA) and for mono-, di-, and triphosphorylated forms of phosphatidylinositol phosphates (PIPs; Figure 2A). No affinity was detected for the nonphosphorylated form of phosphatidylinositol (PI) or for the other 10 membrane lipids present in this blot (Figure 2A). A separate experiment using the START domain of *WKS1.1* (GST-START) showed the same result (Figure 2A).

Based on this result, we selected a more specific lipid blot including PI and seven PIPs at different concentrations. This experiment confirmed the affinity of both *WKS1.1* and *WKS1.2* to mono-, di-, and triphosphorylated forms of PI and their lack of affinity for nonphosphorylated PI (Figure 2B). The interactions with PI(3,4)P₂ and PI(3,4,5)P₃ are not biologically relevant because these PIPs have not been found in plants (Munnik and Vermeer, 2010). Hybridization of the same lipid blot with GST-START domains from both *WKS1.1* and *WKS1.2* showed similar profiles to those obtained from the full-length proteins (Figure 2B). The START domains alone exhibited similar profiles to one another but a relatively weaker affinity for the monophosphorylated forms of phosphatidylinositol than their respective full-length proteins (Figure 2B). Taken together, these results indicate that the lipid binding ability of the full-length *WKS1* protein is most likely mediated by the START domains and that *WKS1.1* and *WKS1.2* have similar lipid binding affinities.

WKS1.1 and WKS1.2 Differ in Their Ability to Form Homodimers

We used a yeast two-hybrid (Y2H) assay to test the ability of *WKS1.1* and *WKS1.2* proteins to form homodimers. Primers for the different Y2H constructs are described in Supplemental Table 2. We first confirmed that no construct shows autoactivation when tested against an empty bait or prey vector (e.g., *WKS1.1* shown in Figure 3B). The full-length *WKS1.1* protein formed homodimers on yeast minimal media/synthetic defined medium (SD) lacking leucine, tryptophan, and histidine (SD -L -W -H) even at the 1:500 dilution (Figures 3C and 3D), but no interaction was detected in the more stringent SD medium lacking also adenine (SD -L -W -H -A; Figures 3C and 3D). By contrast, homodimers were not detected for *WKS1.2*, even in the less stringent SD -L -W -H medium (Figure 3D). Weak interactions were detected between *WKS1.1* and *WKS1.2* proteins (Figure 3C).

To determine the *WKS1.1* regions responsible for the protein-protein interactions, we subcloned the kinase domain alone (KA), the kinase with the interdomain region (KI), the START domain

Table 1. Transgenic Wheat Plants Used in This Study

Construct	Target Gene	Vector Backbone	Promoter	Transformation Method	Bact. Selection ^a	Plant Selection	Host Variety	Purpose
NP:WKS1.1	<i>WKS1.1</i>	pRLF10	Native WKS1 ^b	Agro	amp 100, kan 20	G418	<i>T. aestivum</i> Glasgow	Function of transcript variant
NP:WKS1.2	<i>WKS1.2</i>	pRLF10	Native WKS1 ^b	Agro	amp 100, kan 20	G418	<i>T. aestivum</i> Glasgow	Function of transcript variant
Ubi:TAP-WKS1.1	<i>WKS1.1</i>	pCAMBia1300 ^c	Maize Ubi	Bombardment	kan 50	Bialaphos	<i>T. aestivum</i> Bobwhite	ColP
NP:WKS1.1-GFP	<i>WKS1.1</i>	pGWB4 ^d	Native WKS1 ^b	Bombardment	kan 50	Bialaphos	<i>T. aestivum</i> Bobwhite	Subcellular localization
NP:GFP	<i>GFP</i>	pGWB4 ^d	Native WKS1 ^b	Bombardment	kan 50	Bialaphos	<i>T. aestivum</i> Bobwhite	Subcellular localization control

^aamp, ampicillin; kan, kanamycin.

^bNative WKS1 promoter includes 3543 bp upstream from starting codon.

^cRohila et al. (2006).

^dNakagawa et al. (2007).

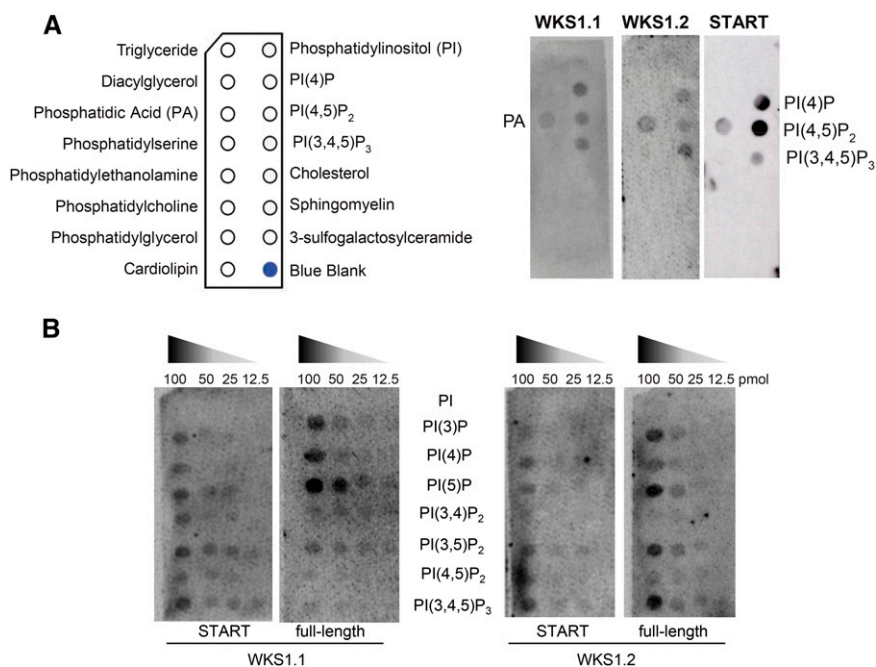


Figure 2. Binding of GST-Tagged WKS1.1 and WKS1.2 Proteins and Their Respective START Domains to Lipid Blots.

(A) Lipid blot with general membrane lipids. The schematic panel to the left indicates the positions of different lipids in the membrane. Membranes hybridized with GST-WKS1.1, GST-WKS1.2, and GST-START domain (from WKS1.1).

(B) Lipid blot with decreasing concentrations of PI and other PIPs evaluated with full-length GST-WKS1.1 and GST-WKS1.2 proteins and their corresponding GST-START domains.

alone (SA), and the interdomain region with the START domain (IS) (Figure 3A). Proteins encoded by the KA and KI constructs interacted with the full-length WKS1.1 (Figure 3C) and formed homodimers in both selection media (Figure 3D). The peptide including the START domain alone was not able to interact with the full-length WKS1.1 and was unable to form homodimers (Figures 3C and 3D). By contrast, the protein including the interdomain and the START domain (IS) was able to interact with WKS1.1 and to form homodimers in both selection media (Figures 3C and 3D). Based on these results, we concluded that the kinase domain is sufficient for dimerization and that the presence of the interdomain region enhances the formation of homodimers.

We also studied the effect on dimerization of four mutations in the kinase domain (*wks1a-d*) and one in the START domain (*wks1e*) of WKS1.1 (Supplemental Figure 3A) that result in complete *Pst* susceptibility (Fu et al., 2009). Mutations *wks1a* and *wks1b* had small effects on the interactions with the full-length wild-type WKS1.1, but showed noticeable reductions in their ability to form homodimers (Supplemental Figures 3B to 3D). By contrast, kinase mutations *wks1c* and *wks1d* significantly reduced the ability of the mutant protein to interact with the wild-type WKS1.1, and mutant homodimers were not detected (Supplemental Figures 3B to 3D). The *wks1e* mutation in the START domain showed an interaction profile similar to that observed for the *wks1c* and *wks1d* kinase mutations (Supplemental Figure 3E). Based on these results, we concluded that all five loss-of-function mutations either reduce or eliminate the ability of WKS1.1 to form homodimers.

WKS1.1 and WKS1.2 Differ in Their Ability to Bind Interacting Proteins

The screening of a Y2H cDNA library from *Pst* infected leaves of tetraploid wheat (Yang et al., 2013) using both full-length WKS1 and kinase interdomain (KI) constructs as bait yielded 16 positive clones under stringent (SD -L -W -H -A) selection. Ten of these clones showed autoactivation and were discarded. Among the remaining six clones, three encoded a wheat thylakoid-associated ascorbate peroxidase (Danna et al., 2003) (henceforth, tAPX), two encoded a vesicle-associated protein 1-3-like (henceforth, VAP1-3), and one encoded an inositol hexakisphosphate and diphosphoinositol-pentakisphosphate kinase 1-like protein (henceforth, PPIP5K1-like) (Supplemental Table 3). For tAPX and VAP1-3, we cloned the full-length coding regions from diploid wheat *Triticum monococcum* and used them to validate the Y2H interactions with WKS1.1 (Supplemental Figure 4 and Supplemental Table 3). The WKS1 interaction with PPIP5K1-like was validated with the original positive clone found in the Y2H screen, which includes only the last three exons of the coding region (Supplemental Figure 4 and Supplemental Table 3).

The three interactors detected in the Y2H screen were also tested for interactions with WKS1.2, the partial KI protein, and the five *wks1a-e* mutants (Supplemental Figure 4 and Supplemental Table 3). All three proteins interacted with KI and WKS1.1, confirming the results from the original screening and the importance of the kinase in these interactions. The interactions of tAPX and VAP1-3 with KI were stronger than those with the complete

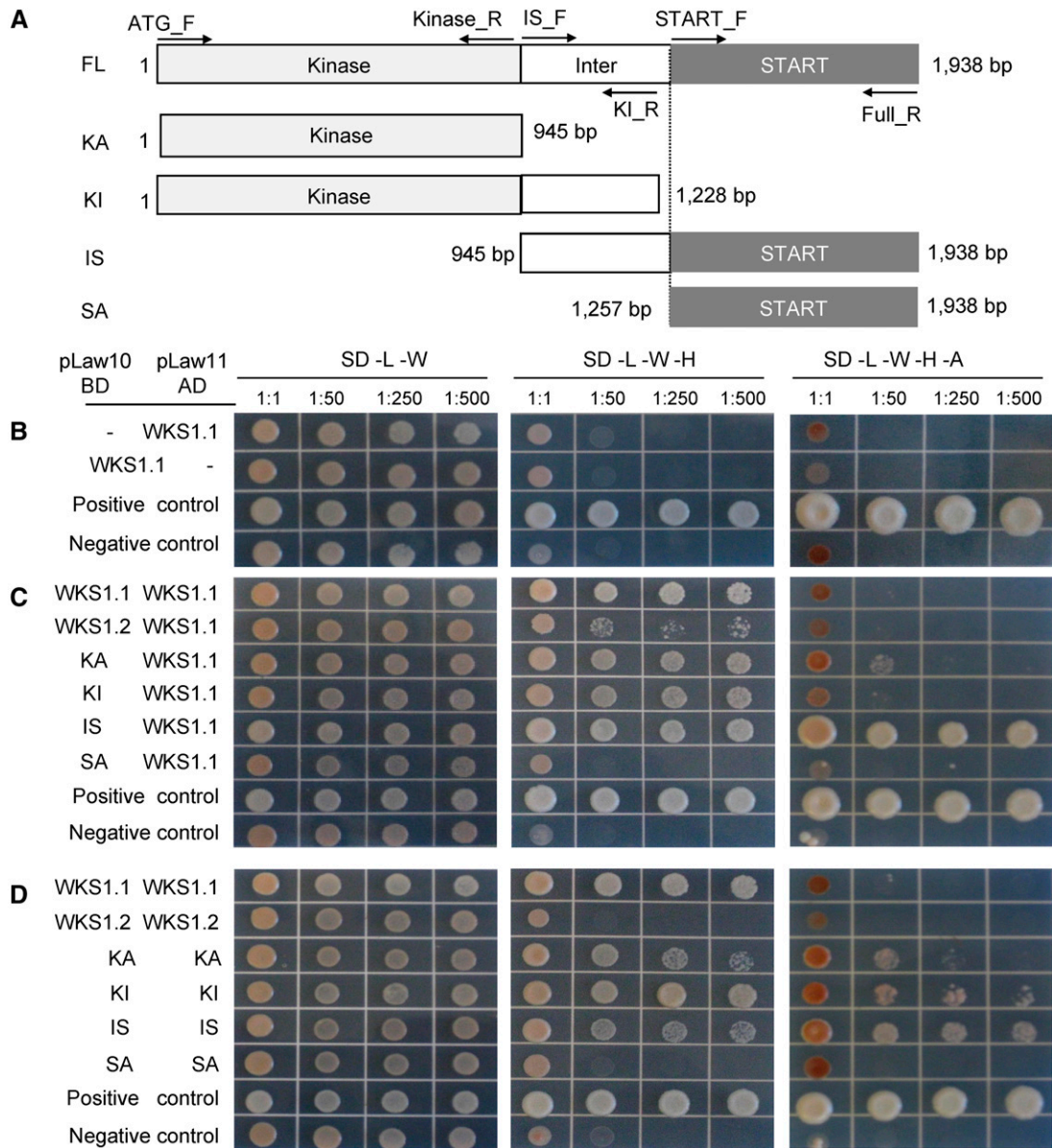


Figure 3. Homodimerization of WKS1.1 and WKS1.2 in Y2H Assays Using Complete and Partial Protein Segments.

(A) Protein regions used in Y2H assays: full-length (FL), kinase domain alone (KA), kinase with interdomain (KI), interdomain with START domain (IS), and START domain alone (SA). Primers are indicated by horizontal arrows and listed in Supplemental Table 2.

(B) WKS1.1 autoactivation test. BD, binding domain; AD, activation domain.

(C) Interaction between complete WKS1.1 and complete WKS1.2 or truncated WKS1 proteins.

(D) Homodimerization of WKS1 domains.

(B) to **(D)** Positive control = pGBKT7-53/pGADT7-T; negative control = pLAW10/pLAW11. See Supplemental Figure 3 for mutants and Supplemental Figure 5 for control protein gel blots.

WKS1.1 protein. None of the three proteins identified in the Y2H screen were able to interact with WKS1.2 or with the mutant proteins *wks1c*, *wks1d*, or *wks1e* (Supplemental Figure 4 and Supplemental Table 3). Protein gel blot analysis confirmed that WKS1.2 and mutant *wks1* proteins were not degraded in the Y2H assays showing no positive interactions (Supplemental Figure 5).

However, a lower level of protein was observed for WKS1.2 and mutant WKS1.1c (Supplemental Figure 5), which may have contributed to the failure to detect positive interactions. Mutant proteins *wks1a* and *wks1b* exhibited detectable interactions with tAPX, VAP1-3, and PPIP5K1-like, but they were weaker than with wild-type WKS1. The only exception was the PPIP5K1-like

interaction with *wks1b*, which was as strong as the interaction with the wild-type *WKS1*. These interactions parallel the results from the homodimerization tests (Supplemental Figure 3), suggesting that the formation of *WKS1.1* homodimers may favor the interactions between *WKS1.1* with *tAPX*, *VAP1-3*, and *PPIP5K1*-like proteins.

The Y2H interaction between *tAPX* and *WKS1.1* was validated using a bimolecular fluorescence complementation assay in *Nicotiana benthamiana* (Supplemental Figure 6). Cells from *N. benthamiana* epidermal layer have very few or no chloroplasts so the observed cytoplasmic localization is not unexpected. In addition, the fusion of YFP (yellow fluorescent protein) to the N-terminal region of *tAPX* may have also interfered with its chloroplast localization signal. The interaction between *tAPX* and *WKS1.1* was further validated in wheat plants by coimmunoprecipitation (CoIP) (Figure 4). Using a commercial rabbit *tAPX* antibody, we detected a specific band of ~40 kD in pull-down samples from the transgenic plants overexpressing *TAP-WKS1.1*, but not in those from the nontransgenic control (Figure 4). The size of this band corresponds with the expected size of a mature wheat *tAPX* protein (40.2 kD). This last experiment confirmed that the interaction between *WKS1.1* and *tAPX* detected in yeast and in *N. benthamiana* also occurs in wheat plants. Since *tAPX* is a well-characterized chloroplast protein (Shigeoka et al., 2002), this result suggests that *WKS1.1* has a chloroplast localization.

WKS1.1 Is Targeted to Chloroplasts

To determine the subcellular localization of *WKS1.1* in wheat cells *in vivo*, we generated stable transgenic wheat plants expressing the coding sequence of *WKS1.1* fused with the green fluorescent protein (GFP) under the control of the *WKS1* native promoter (NP:*WKS1.1*-GFP). As a negative control, we also generated

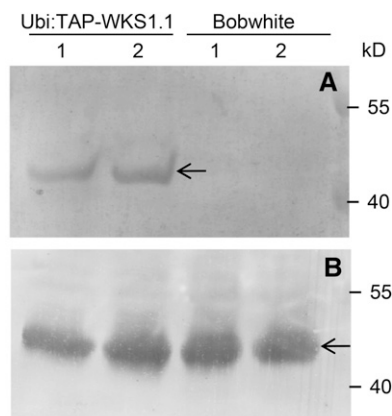


Figure 4. In Planta Interaction between *WKS1.1* and *tAPX*.

(A) CoIP of *WKS1.1* and *tAPX1* in Bobwhite control (no-*WKS1*) and transgenic plants overexpressing *TAP-WKS1.1* fusion protein. The arrow indicates the position of the mature *tAPX1* protein detected by anti-*tAPX* rabbit antibody. 1 and 2 indicate samples from different transgenic events and from two different control plants (biological repeats).

(B) Loading control. Total protein from *TAP-WKS1.1* transgenic plants and Bobwhite control analyzed with anti-*tAPX* rabbit antibody. All CoIP assays were performed with equal amounts of total protein (measured with a BCA protein quantification kit; Yeasen).

stable transgenic plants expressing GFP alone under the control of the same promoter (NP:GFP) (Table 1). As expected, no GFP fluorescence was observed in the nontransgenic Bobwhite (Figure 5A), and fluorescence was detected in the cytoplasm in the NP:GFP transgene control (Figure 5B). In two independent transgenic lines expressing the *WKS1.1*-GFP fusion protein, fluorescence was detected in the chloroplasts of mesophyll cells where it colocalized with chlorophyll autofluorescence (Figures 5C and 5D).

The Bobwhite transgenic plants transformed with the *WKS1.1*-GFP construct were all susceptible to *Pst* (Supplemental Figure 7A). This result differed from the partial resistance to *Pst* observed in the wheat plants transformed with NP:*WKS1.1* (Figures 1F and 1G; Fu et al., 2009) or Ubi:*TAP-WKS1.1* (Supplemental Figure 7B). To explore the possible causes for these differences, we tested the effect of GFP and TAP tags at the N and C terminus of *WKS1.1*. The addition of GFP or TAP tags at the C terminus of *WKS1.1* blocked its ability to form homodimers and to interact with *tAPX* in Y2H assays (Supplemental Figure 7B). When the tags were placed in the N terminus of *WKS1.1*, we obtained different results in the Y2H assays. *TAP-WKS1.1* showed homodimers and a strong interaction with the full-length *tAPX*, but *GFP-WKS1.1* showed weak homodimer formation and no interaction with *tAPX*. These results suggest that a disruption of the C-terminal region of *WKS1.1* does not affect its subcellular localization but can have a negative impact on *WKS1.1* protein interactions and its ability to confer resistance to *Pst*.

To provide further support for *WKS1.1* localization to chloroplasts, we performed *in vitro* import assays using chloroplasts isolated from pea (*Pisum sativum*) seedlings and radiolabeled *WKS1.1* protein with or without a GFP tag. When the nontagged *WKS1.1* was examined by the assay, three major bands of 72, 66, and <50 kD were recovered in the integral membrane fraction, which was obtained by centrifugation after lysis with an alkaline buffer (Figure 6A, lane 4). Among the recovered proteins, the 72-kD band appears to correspond to the full-length *WKS1.1* translation product (Figure 6A, lane 1). A chloroplast-import time-course assay showed the increase of the 66-kD band from 3% of the total *WKS1.1* protein after 5 min to 25% after 40 min (Figure 6B, compare lanes 2 and 5). These results suggest that the 66-kD band was derived from the 72-kD protein during the assay; thus, we named it as mature-*WKS1.1* (M-*WKS1.1*). Postimport treatment of chloroplasts with thermolysin, a protease that has access to surface-exposed proteins (Cline et al., 1984), resulted in degradation of the 72-kD band but M-*WKS1.1* remained intact (Figure 6A, lane 6). The activity of the protease in the assay was confirmed by treating an aliquot of the same sample in the presence of detergent (Figure 6A, lane 7). Additional controls included assays without detergent using an outer membrane protein DGD1 (Froehlich et al., 2001), which was digested (Supplemental Figure 8, lane 4), and an inner membrane protein Tic40 (Stahl et al., 1999), which was resistant (Supplemental Figure 8, lane 9). Figure 6C shows that the larger fusion protein *WKS1.1*-GFP is also imported into the chloroplast. As in the nontagged *WKS1.1*, the imported protein (resistant to thermolysin) migrated slightly faster (~6 kD) than the precursor protein used for the assay. These data suggest that the ~6-kD truncation occurs in the N terminus of *WKS1.1*. The START domain alone was also recovered in the chloroplast

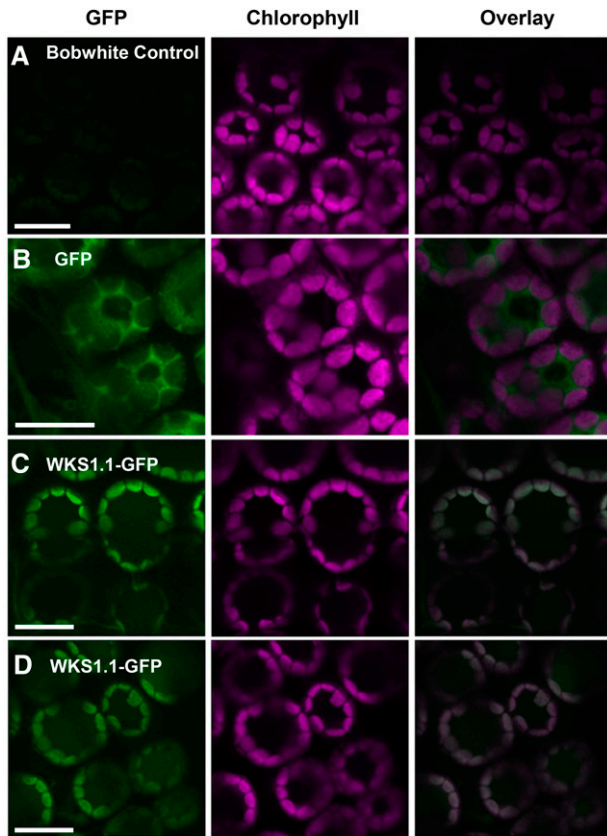


Figure 5. WKS1.1 Is a Chloroplast Protein in Wheat.

(A) Background fluorescence of nontransgenic Bobwhite control. Bar = 10 μm .

(B) Green fluorescence of free GFP in transgenic Bobwhite is observed in the cytosol (surrounding the chloroplasts and the central vacuole). Bar = 10 μm .

(C) and (D) Green fluorescence of WKS1.1-GFP fusion in transgenic wheat lines AB53-81a-2-4 and AB-53-62a-1-2 colocalizes with chlorophyll autofluorescence in chloroplasts. Bar = 10 μm .

integral membrane fraction (Figure 6D, lane 4) but was degraded by thermolysin (Figure 6D, lane 6). Taken together, these results confirm the chloroplast localization of WKS1.1. They also show that the START domain may play a role in WKS1.1 targeting of the chloroplast but that it is not sufficient to be imported into the chloroplast when separated from the N terminus of WKS1.1.

WKS1.1-Kinase Phosphorylates tAPX Protein in Vitro and in Planta

To test if WKS1 phosphorylates tAPX, we first purified the kinase portion of WKS1 (KA) and the full-length tAPX using a 6X His tag. We then incubated tAPX with KA and ATP, and samples lacking tAPX or ATP as negative controls. We then stained the extracted proteins with a fluorescent dye that specifically binds to phosphorylated peptides. The fluorescence bound to the protein was significantly higher in the samples with ATP than in the samples without ATP ($P < 0.0001$; Figure 7A), confirming the

presence of phosphorylated peptides. In the presence of ATP, the samples with both KA and tAPX showed significantly higher fluorescence than the sample with KA alone ($P < 0.05$; Figure 7A), suggesting tAPX phosphorylation. However, high levels of fluorescence were also detected in the sample containing KA without tAPX, indicating that the WKS1-kinase is capable of autophosphorylation.

To confirm the WKS1-kinase phosphorylation of tAPX, we used two different *in vitro* assays. First, we performed the kinase reaction with radioactive [γ - ^{32}P]ATP, WKS1-kinase, and tAPX and separated the products by SDS-PAGE. As a control, we used a similar sample replacing tAPX by PPIP5K1-like, which is not phosphorylated by WKS1-kinase. Both samples showed a strong signal for a small band corresponding to the autophosphorylated WKS1-kinase (Figure 7B, arrowhead), but only the sample with the tAPX protein showed an additional phosphorylated product of the size expected for tAPX (Figure 7B, lane 2, arrow). We then used a Phos-tag SDS-PAGE retardation assay. The tAPX protein from the samples with the WKS1-kinase and ATP showed retardation relative to the samples without ATP (Figure 7C). Taken together, these experiments indicate that the WKS1-kinase is able to phosphorylate tAPX *in vitro*.

To test the ability of WKS1 to phosphorylate tAPX *in planta*, we first extracted intact chloroplasts from nontransgenic wheat variety Bobwhite (control without *WKS1*) and from three independent transgenic Bobwhite plants previously transformed with a genomic copy of *WKS1* (Fu et al., 2009). In a Phos-tag SDS-PAGE retardation assay using the tAPX antibody, we observed that the tAPX proteins extracted from intact chloroplasts from the three independent Bobwhite-WKS1 transgenic plants were retarded compared with the sample from the nontransgenic Bobwhite control (Figure 7D). This result supports the hypothesis that WKS1 is targeted to the wheat chloroplast and phosphorylates tAPX *in planta*.

WKS1.1 Reduces tAPX Activity in Vitro and in Planta

To address the consequence of tAPX phosphorylation, we first investigated the biochemical characteristics of the *T. monococcum* tAPX protein. The activity of the recombinant tAPX protein prepared from *Escherichia coli* was significantly increased ($P < 0.001$) in the presence of 5 mM MgCl_2 and greatly reduced ($P < 0.001$) in the presence of CaCl_2 and FeCl_3 compared with a buffer with no additional ions (Supplemental Figure 9A). The tAPX protein had peroxidase activity in a wide range of pHs (5.0 to 8.0) with an optimum at 6.0 (Supplemental Figure 9B). Further tAPX activity experiments used pH 6.0 and a 5 mM MgCl_2 concentration.

An equal amount of tAPX recombinant protein was mixed for 3 h with WKS1.1-kinase/ATP, GST/ATP (negative control), or WKS1.1-kinase without ATP, and the activity of tAPX was quantified. tAPX samples mixed with GST/ATP or with WKS1.1 protein without ATP had similar tAPX-specific activity (1.54 versus 1.57 nmol ascorbic acid $\text{min}^{-1} \mu\text{g protein}^{-1}$, *t* test, $P = 0.91$), indicating that the physical binding of WKS1 with tAPX has little effect on tAPX activity (Figure 8A). However, in the samples including both WKS1.1 protein and ATP, tAPX activity was reduced by roughly 40% ($P < 0.05$; Figure 8A). This result indicates that the phosphorylation by WKS1.1 reduces tAPX activity *in vitro*.

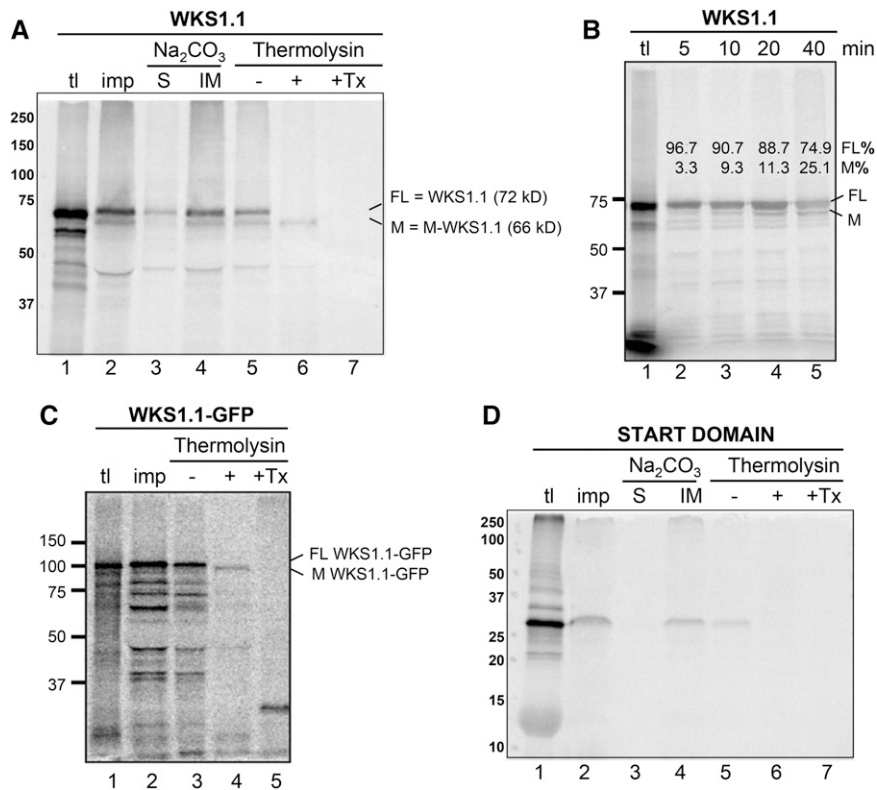


Figure 6. WKS1.1 Chloroplasts Import Assays.

(A) Radiolabeled full-length WKS1.1 protein incubated with intact chloroplasts. tl = 10% of translation products used for the import assay; imp. = proteins in intact chloroplasts recovered after a 20-min import reaction; Na_2CO_3 = chloroplasts lysed with 0.1 M Na_2CO_3 and fractionated by centrifugation into a supernatant that contained soluble proteins (S) and a pellet that contained integral membrane proteins (IM); thermolysin = chloroplasts incubated on ice for 30 min without (–) or with (+) thermolysin, or with thermolysin and 2% (v/v) Triton X-100 (Tx). Radiolabeled proteins were visualized using a phosphor imager: FL; full-length WKS1.1 (72 kD); M, processed M-WKS1.1 (66 kD).

(B) Radiolabeled full-length WKS1.1 protein incubated with intact chloroplasts for the time indicated at the top of the gel and analyzed as described in the legend of **(A)**. Intensity of each band relative to the total WKS1.1 protein (FL+M) is indicated above the bands.

(C) and **(D)** Radiolabeled WKS1.1-GFP fusion protein **(C)** and radiolabeled START domain protein **(D)** incubated with intact chloroplasts and analyzed as described in the legend of **(A)**.

The sizes of molecular mass markers in kilodaltons are shown to the left of each image. Import of control proteins DGD1 (located at the outer membrane) and Tic40 (located at the inner membrane) can be found in Supplemental Figure 8.

To confirm these results in planta, we measured APX activity in soluble and thylakoid fractions extracted from leaves of Bobwhite plants transformed with either NP:GFP (control) or NP:WKS1 (independent transgenic lines 26b-15, 26b-6, and 17a-15; Fu et al., 2009). The three NP:WKS1 transgenic plants showed significantly lower APX activity than the control in the thylakoid fraction (31 to 49% reduction, $P < 0.05$ one event and $P < 0.01$ two events; Figure 8B). No significant difference in APX activity was detected between genotypes in the soluble fraction (Figure 8C), suggesting that the reduced APX activity is specific to the thylakoid-associated tAPX.

To test if a reduction in tAPX activity independent of WKS1 can contribute to *Pst* resistance, we used a wheat line carrying a deletion of the B-genome copy of *tAPX*, henceforth referred to as $\Delta tAPX-6B$ (Danna et al., 2003). This mutation was previously associated with a reduction in total tAPX activity and with reduced photosynthetic activity and biomass accumulation under

high light intensity (Danna et al., 2003). We crossed this mutant with the Ubi:TAP-WKS1.1 transgenic Bobwhite, self-pollinated the F1 hybrid, and generated an F2 population segregating for Ubi:TAP-WKS1.1 and $\Delta tAPX-6B$. Plants carrying the WKS1.1 transgene showed partial resistance to *Pst*, whereas those without this transgene were susceptible (Figure 8D). The presence or absence of the $\Delta tAPX-6B$ mutation did not alter significantly the reaction to *Pst* in the plants with (partial resistance) and without WKS1.1 (susceptible; Figure 8D). This result suggests that the reduction of tAPX activity conferred by the $\Delta tAPX-6B$ mutation in this experiment was not sufficient to enhance resistance to *Pst*.

Transgenic Wheat Lines with Multiple WKS1 Copies Show Accelerated Leaf Senescence

In the original study of *WKS1* (Fu et al., 2009), we noticed that some of the *Pst*-resistant transgenic wheat plants that contained

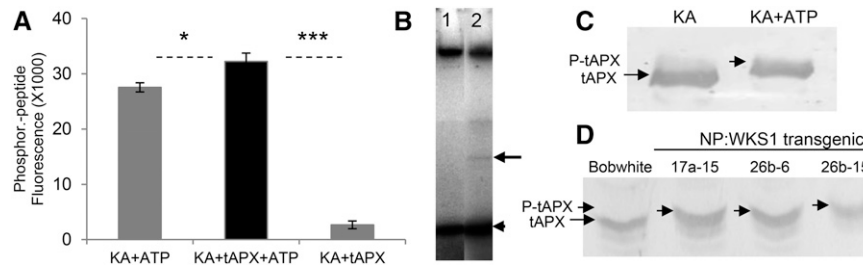


Figure 7. WKS1-Kinase Phosphorylates tAPX Protein in Vitro and in Vivo.

(A) Phosphofluorescence generated by autophosphorylation of the WKS1-kinase domain (KA+ATP) and by additional phosphorylation of tAPX by KA (KA+tAPX+ATP). The KA+tAPX control contained no ATP. Data represent the mean of five replications, and error bars are standard errors of the means. * $P < 0.05$ and *** $P < 0.001$.

(B) Phosphoimage of PPIP5K-like (lane 1, control) and tAPX (lane 2), both incubated with WKS1-kinase domain (KA) and [γ - 32 P]ATP. The arrow indicates the phosphorylated tAPX and the arrowhead the autophosphorylated KA. PPIP5K protein is not phosphorylated by KA.

(C) Gel retardation of tAPX protein after WKS1-kinase phosphorylation initiated by ATP addition. tAPX was detected by anti-APX antibody. tAPX and P-tAPX indicate the position of tAPX protein before and after phosphorylation, respectively.

(D) Immunoblot of Phos-tag SDS-PAGE of proteins extracted from chloroplasts of nontransformed Bobwhite and three different transformants containing NP:WKS1 (17a-15, 26b-6, and 26b-15). Proteins were detected with anti-APX antibody.

multiple copies of the *WKS1* genomic region showed earlier senescence of the lower leaves than the nontransgenic control in the absence of the pathogen. To validate this preliminary observation, we selected two independent transgenic events (17a and 26b) with multiple *WKS1* copies and compared two plants of each event with the nontransgenic control. Eight plants from each genotype were grown in a controlled environment chamber under long-day photoperiod (16 h light/8 h dark), and the second leaf of each plant was compared at the same developmental stage. All four transgenic plants showed accelerated senescence compared with the nontransgenic control (Figure 9A).

To quantify these differences in senescence, we measured relative chlorophyll content using a hand-held chlorophyll meter (SPAD-502; Minolta) in the midsection of the different leaves of eight transgenic and eight control plants at the time of ear emergence (10 measurements per individual leaf). Significant reductions in relative chlorophyll content in the three older leaves (Figure 9B, 1st to 3rd leaf, Dunnett's test, $P < 0.01$) were detected in the four transgenic genotypes relative to the nontransgenic Bobwhite control. These results confirmed that the presence of multiple copies of *WKS1* in the Bobwhite plants transformed by bombardment (Fu et al., 2009) is associated with early leaf senescence. Using the Amplex red hydrogen peroxide/peroxidase assay kit (Molecular Probes), we confirmed that the transgenic *WKS1* plants had significantly higher levels of H_2O_2 than the wild-type control (statistical contrast between the wild type and four transgenic lines, $P = 0.011$; Figure 9C).

DISCUSSION

WKS1 Is Targeted to the Chloroplast

The localization of WKS1.1 to the chloroplast was an unexpected result because there are only a few examples of resistance proteins targeted to this organelle, including Arabidopsis RESISTANCE TO

PHYTOPHTHORA1 (Belhaj et al., 2009) and the chloroplastic/cytoplasmic protein NRIP1, which in association with the NB-LRR immune receptor "N" is responsible for *Tobacco mosaic virus* recognition and resistance in *Nicotiana* (Caplan et al., 2008). This chloroplast localization was also unexpected because no chloroplast transit peptide (Shi and Theg, 2013) was predicted for WKS1. However, proteomic studies have shown that ~10% of the chloroplast proteins lack a cleavable transit peptide (Armbruster et al., 2009). Some of these proteins use an alternative chloroplast targeting pathway that involves the endoplasmic reticulum (ER) and the Golgi apparatus (Radhamony and Theg, 2006). However, this pathway may not be relevant for WKS1, which lacks an ER signal peptide and can be imported into purified chloroplasts in vitro.

WKS1 interacts with VAP1-3 (Supplemental Figure 4), which belongs to a class of proteins previously shown to be located in the ER and to be involved in membrane traffic (Loewen and Levine, 2005). We confirmed the interaction between WKS1.1 and VAP1-3 by bimolecular fluorescence in *N. benthamiana* protoplasts (Supplemental Figure 10) and initiated a screen for mutations in wheat VAP1-3 to test if this protein is required for the transport of WKS1.1 to the chloroplast.

Alternative Splice Variants WKS1.1 and WKS1.2 Exhibit Altered Properties and Function

WKS1 is present in several alternative splice variants, including the complete protein (WKS1.1), the major variant WKS1.2 that lacks the last exon, and several less frequent shorter variants (Fu et al., 2009). Alternative splicing is a widespread mechanism in animals and plants that increases diversity of transcripts (e.g., different RNA stability) and proteins (e.g., different subcellular localization, stability, or function) (Syed et al., 2012; Staiger and Brown, 2013). This seems to be also the case for WKS1 alternative splice variants, which differ in their abilities to form homodimers, to interact with other proteins, and to confer resistance to *Pst*. WKS1.2 and the shorter alternative splice variants all lack

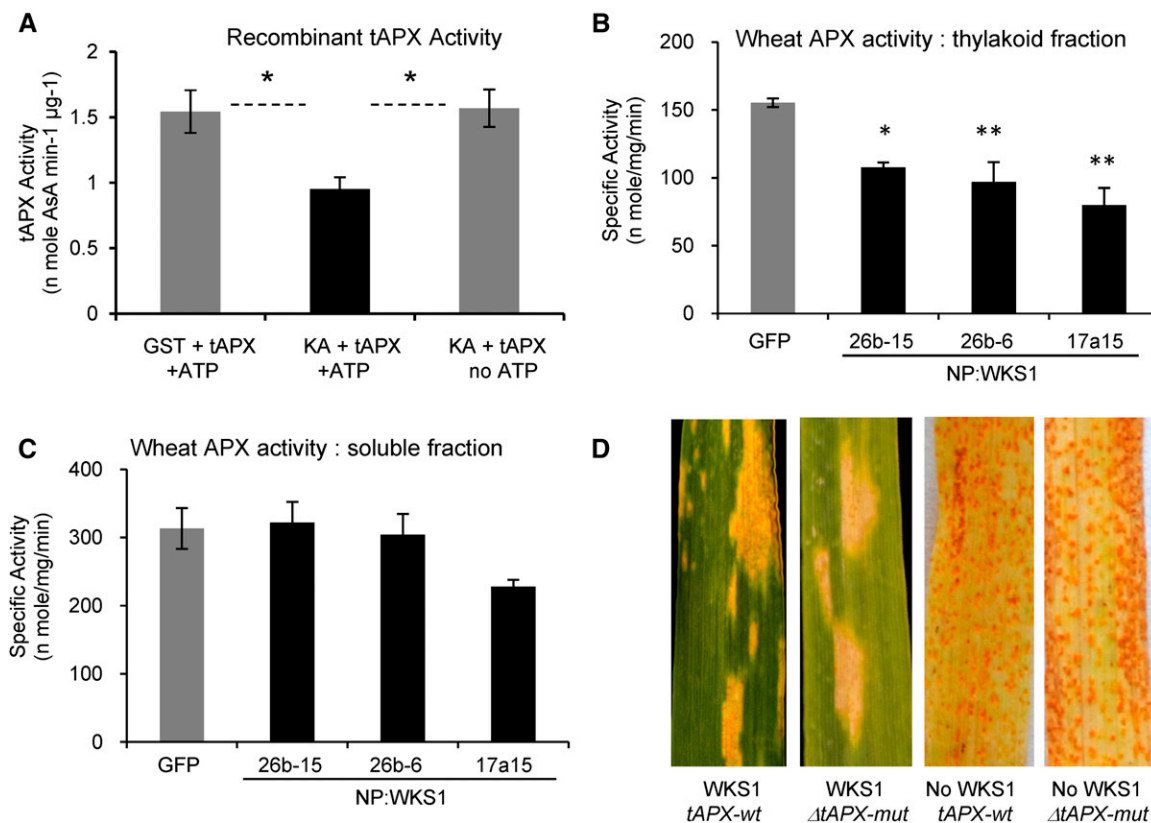


Figure 8. Effect of WKS1.1 on tAPX Activity in Vitro and in Planta.

(A) tAPX-specific activity in the presence of GST+ATP (negative control), KA+ATP, and KA without ATP ($n = 4$, $*P < 0.05$; KA = kinase alone). Error bars are standard errors of the means.

(B) APX-specific activity in thylakoid fractions from Bobwhite plants transformed with NP:GFP (control) and with NP:WKS1 (genomic). Dunnett's tests, $*P < 0.05$ and $**P < 0.01$

(C) APX-specific activity in soluble fractions extracted from the same genotypes as in **(B)**. No significant differences were detected.

(B) and **(C)** 26b15, 26b6, and 17a15 are three independent transformation events with a genomic copy of *WKS1* (Fu et al., 2009). Error bars are standard errors of the means.

(D) F3 families segregating for $\Delta tAPX-6B$ deletion and Ubi:TAP-WKS1.1 transgene infected with *Pst* race PST130. Plants carrying WKS1.1 showed partial resistance and plants without the transgene were susceptible. The $\Delta tAPX-6B$ deletion did not affect *Pst* resistance.

the last 11 amino acids of the START domain, which include several amino acids that are conserved across plants and mosses (Fu et al., 2009). The addition of a GFP tag to the C terminus of WKS1.1 limited the formation of homodimers, the interaction with tAPX, and the resistance to *Pst*, confirming the importance of this region in WKS1.1 function. Since WKS1.1-GFP is imported into the chloroplasts as efficiently as the full-length WKS1.1 (Figure 6C), the *Pst* susceptibility of the wheat plants transformed with WKS1.1-GFP (Supplemental Figure 7A) is most likely due to the inability of WKS1.1-GFP to form homodimers and to interact with tAPX or other proteins (Supplemental Figure 7B).

The C-terminal region of the START domain is also critical for normal function of several human START proteins (Alpy and Tomasetto, 2014). This region includes an α -helix that can interact with lipid membranes and regulate the accessibility of the lipid ligand to the lipid binding pocket (Alpy and Tomasetto, 2014). The truncation of the C-terminal region of the START

domain in WKS1.2 may alter similar functions in wheat, resulting in nonfunctional proteins. Since only WKS1.1 is effective against *Pst*, the increase in *WKS1.1* transcript levels relative to *WKS1.2* during the first 3 d of *Pst* infection (Fu et al., 2009) might have an impact on the resistance response.

WKS1 START Domain Has Lipid Binding Ability

The mammalian START proteins bind diverse ligands, such as cholesterol, oxysterols, phospholipids, sphingolipids, and possibly fatty acids (Clark, 2012), and several of these ligands appear to be shared by plant START domains (Schrick et al., 2014). However, lipid ligands for plant START domains have been studied only for Arabidopsis homeodomain leucine zipper (HD-Zip) transcription factors (Schrick et al., 2014). These START domains are distantly related to the START domain present in Arabidopsis EDR2 (Schrick et al., 2004), which is the

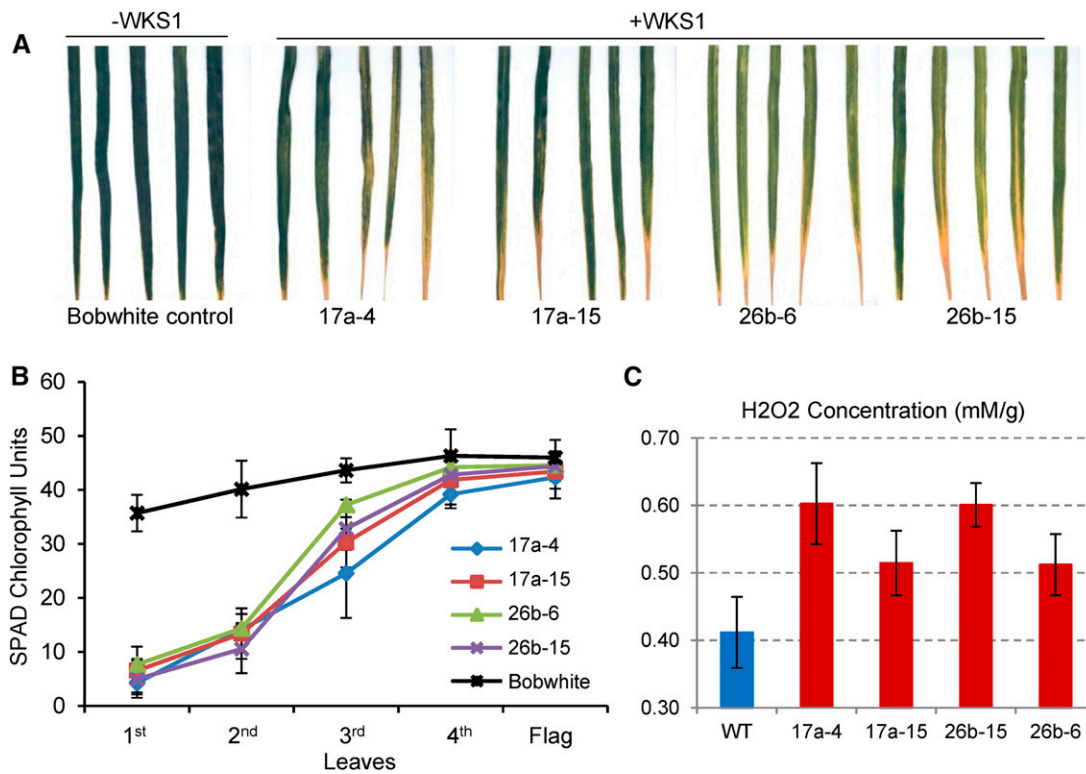


Figure 9. Leaf Necrosis in Transgenic Wheat with Multiple Genomic Copies of *WKS1*.

(A) Early senescence of 2nd leaves of *WKS1* transgenic plants from two independent events (sibs 17a-4 /17a-15 and sibs 26b-6/26b-15) in the absence of *Pst*. Nontransgenic Bobwhite serves as control.

(B) Relative SPAD chlorophyll units of *WKS1* transgenic or Bobwhite control plants. Samples were collected from the midsection of each leaf from the oldest (1st) to the youngest (flag leaf). Data points are means of eight measurements per leaves from 10 individual plants. Error bars are standard errors of the means.

(C) Quantification of H₂O₂ using an Amplex red hydrogen peroxide/peroxidase assay kit (Molecular Probes). Transgenic plants showed significantly higher H₂O₂ levels than the wild-type control (statistical contrast between the wild type and four *WKS1* transgenic lines, $P = 0.011$). Samples were collected from the mid-region of the second oldest leaf from five to nine 5-week-old plants per genotype (growth conditions: 16 h light at 25°C and 8 h dark at 20°C). Error bars are standard errors of the means.

closest to the *WKS1* START domain (Fu et al., 2009). The START domain of EDR2 is more closely related to the human STARD14/D15 subfamily than to the plant START domains in the HD-Zip transcription factors (Schrick et al., 2004), which suggests that this START domain group likely originated before the divergence of plants and animals. Similarly to *WKS1*, STARD14 active form is a dimer and presents alternative splicing forms with distinct START domain C-terminal ends (Alpy and Tomasetto, 2014).

The lipid blots analyzed here showed that the START domain from *WKS1* has affinity for PA and several PIPs (Figure 2A). START domains of Arabidopsis HD-Zip transcription factors PDF2 and GL2 also show affinity for PA, among various other phospholipids, but affinity for PIPs has not been described to our knowledge for other plant or animal START domains (Alpy and Tomasetto, 2014; Schrick et al., 2014). We currently do not know if this is because *WKS1.1* START domain has a unique lipid affinity or because PIPs have not been extensively tested in START domain binding assays (Schrick et al., 2014). Both PA and PIPs are important molecules in cellular signaling and

trafficking (Munnik and Vermeer, 2010; Testerink and Munnik, 2011) and have been implicated in plant disease resistance (de Jong et al., 2004; Park et al., 2004; Andersson et al., 2006; Raho et al., 2011; Hung et al., 2014). It would be interesting to investigate if there is a connection between the ability of *WKS1* to bind PA and PIPs and its ability to detect the presence of *Pst*.

***WKS1* Phosphorylation of tAPX Is Associated with H₂O₂ Accumulation and Cell Death in *Pst*-Infected Regions**

In the absence of the pathogen, the wild-type allele of *WKS1* seems to have a limited negative effect on yield performance of hexaploid wheat, since near-isogenic lines differing in the presence of *WKS1* and the tightly linked *GPC-B1* gene showed no significant yield differences in multiple environments (Brevis et al., 2008). However, compared with the nontransgenic control, transgenic wheat plants transformed by bombardment and including multiple genomic copies of *WKS1* (Fu et al., 2009) showed premature senescence of the older leaves (Figures 9A and 9B),

which was associated with significantly higher levels of H_2O_2 (Figure 9C). Rapid increases in ROS levels play an important role in disease resistance by triggering cell death near infection sites and thereby limiting pathogen proliferation (Bradley et al., 1992; Levine et al., 1994; Greenberg, 1996).

tAPX plays a central role in the detoxification of H_2O_2 generated during photosynthesis. Using the reducing power of ascorbate and other endogenous antioxidants, tAPX catalyzes the reduction of H_2O_2 to water (Caverzan et al., 2012). Arabidopsis tAPX knockout mutants show significantly higher levels of H_2O_2 than the wild type after exposure to intense light (Maruta et al., 2010). Similarly, hexaploid wheat plants lacking the tAPX-6B homoeolog show reduced photosynthesis and increased susceptibility to rapid oxidative stress (Danna et al., 2003). Based on the previous observations, we hypothesize that the reduced tAPX activity in planta observed in the presence of WKS1.1 contributes to the accumulation of H_2O_2 and the initiation of the progressive cell death response characteristic of the WKS1.1 partial resistance reaction to *Pst* (Figure 1).

Since programmed cell death, developmental senescence, and responses to pathogens are linked through complex genetic regulatory networks (Pavet et al., 2005; Feng et al., 2014), we also evaluated the effect of the $\Delta tAPX-6B$ mutation on the modulation of the *WKS1.1* responses to *Pst*. The deletion of one of the three tAPX homoeologs in hexaploid wheat ($\Delta tAPX-6B$) was not sufficient to confer resistance to *Pst* in the absence of *WKS1.1*. This result suggests that the *WKS1* mechanism to detect *Pst* is more complex than a simple reduction in the threshold of ROS-induced senescence and may involve the detection of changes in PA or PIP signaling through the START domain or interactions with other pathogen or wheat proteins. Among the plants carrying *WKS1.1*, the presence of the $\Delta tAPX-6B$ mutation was not associated with obvious differences in the levels of resistance (Figure 8D). However, it is important to consider that these observations were made in an F2:3 population that was still segregating for flowering time and other traits. The detection of subtle differences in *Pst* resistance or H_2O_2 accumulation associated with the $\Delta tAPX-6B$ mutation will require further experiments in a uniform genetic background.

A Working Model for WKS1 Partial Resistance Mechanism

Figure 10 summarizes our current working model for the role of *WKS1* in the induction of cell death. Previous results have shown that *Pst* infection triggers an increase in *WKS1.1* and a decrease in *WKS1.2* transcripts levels (Fu et al., 2009). According to this working model, the increased levels of the functional *WKS1.1* variant result in increased phosphorylation of tAPX, reduced tAPX activity, and reduced ability of the cells to detoxify ROS. The gradual accumulation of ROS ultimately results in cell death and partial resistance to *Pst*. The *WKS1*-mediated resistance process takes approximately 1 week to contain the progression of the *Pst* infection (Supplemental Figure 1). This is several days longer than previously described hypersensitive responses to *Pst* triggered by *R* genes, which result in necrotic cells within 2 to 4 dpi (Wang et al., 2007). The slower resistance response associated with *WKS1* allows some

Pst intercellular growth and sporulation and results in a partial resistance response (Figure 1; Supplemental Figure 1).

Although the role of the START domain in this mechanism is still not clear, we know that this domain is required for *Pst* resistance, since a single amino acid mutation in the hydrophobic pocket of the START domain in the *wks1e* mutant (Fu et al., 2009) or the addition of a GFP tag at the C-terminal end of the START domain (Supplemental Figure 7A) results in complete susceptibility. One possible role of the START domain is to modulate *WKS1* ability to form homodimers and to interact with tAPX and other downstream proteins. Ligand binding by the START domain has been also proposed as a mechanism to regulate the activities of adjacent domains, such as Rho-GAP and thioesterase domains in the human START domain-containing protein STARD14 (Schrack et al., 2014). Results from Figure 3D are consistent with this hypothesis: The kinase domain without the START domain is able to form homodimers in the stringent Y2H assays (SD -L-W-H-A), but the complete *WKS1.1* protein domain can form homodimers only under low stringency Y2H assays (SD -L-W-H; Figure 3D). These results suggest that, under certain physiological conditions, the presence of the START domain can reduce the strength of the protein-protein interactions mediated by the kinase and the interdomain.

The particular *Pst* resistance mechanism described here for *WKS1.1* may have implications in the utilization of this gene in agriculture. The combination of resistance genes with different modes of action against the same pathogen has been proposed as a strategy to extend the durability of deployed resistance genes (Lowe et al., 2011). In this context, *WKS1.1* is an interesting candidate for deployment in gene pyramids with other *Pst* resistance genes. Only the test of time will determine if this strategy will result in more stable resistance against this devastating pathogen.

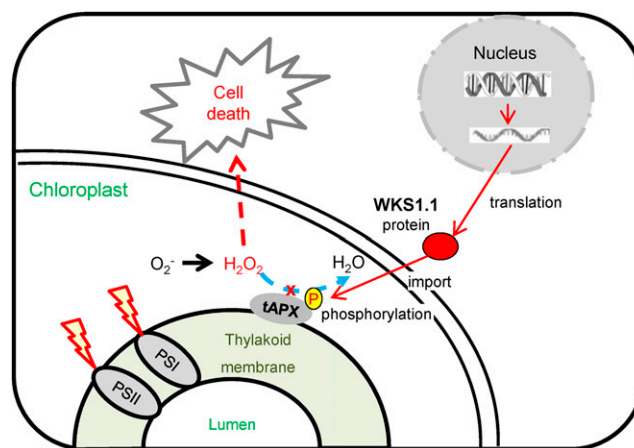


Figure 10. Working Model of *WKS1.1* Regulation of Cell Death.

The *WKS1.1* protein is imported into the chloroplast, where it phosphorylates tAPX, reducing its ability to detoxify the H_2O_2 generated by photosynthesis. The dotted blue line indicates reduced peroxidase activity, and the dotted red line indicates increased H_2O_2 concentration, which causes cell death. PSI, photosystem I; PSII, photosystem II.

METHODS

Plant Materials

Hexaploid wheat (*Triticum aestivum*) breeding line UC1041 and a near isogenic line with the *WKS1* gene, together with two previously described homozygous *WKS1*-kinase mutants *wks1b* and *wks1d* (susceptible) and their respective wild-type sister controls (resistant) (Fu et al., 2009), were used for the *Pst* infection time course. Methods used for the evaluation of the different stages of *Pst* infection are described in detail in Supplemental Methods 1. All the chamber experiments were conducted under a long-day photoperiod (16 h light/8 h dark). For the stripe rust inoculations, plants were placed in a dew chamber without light at 10°C for 24 h. Plants were inoculated, transferred to 25°C, and then evaluated for resistance (3, 6, 10, and 13 dpi for the time-course experiment).

The hexaploid wheat varieties 'Glasgow' and 'Bobwhite' were used for the transformation experiments. The specific genes, promoters, vectors, and selection methods used for each variety are summarized in Table 1, in the transgenic method section below, and in Supplemental Methods 2.

A deletion mutant of the B-genome copy of *tAPX* in the hexaploid wheat variety 'Sinalocho MA,' kindly provided by R.A. Ugalde from the Instituto Nacional de Tecnología Industrial, Argentina (Sacco et al., 1998), was crossed with a transgenic Bobwhite overexpressing *WKS1* (Ubi:TAP-WKS1) to study the effect of *WKS1* on *tAPX* in planta. The hybrid was self-pollinated, and sister lines homozygous for the *tAPX-6B* deletion, the *WKS1.1* transgene, or for both were selected from the segregating F2 plants using primers UbiP-F1 and TAP-R254 for Ubi:TAP-WKS1.1, and TAPX-6B-F and TaAPX-6B-R for the *tAPX-6B* deletion (Supplemental Table 2). Plants were inoculated with *Pst* race PST130 at 10°C and then transferred to 25°C and evaluated for resistance 3 weeks later.

Wheat Transformation

To characterize the effect of *WKS1* on leaf senescence, we used transgenic plants that carry a complete genomic copy of *WKS1* including 3.5-kb region upstream from the start codon and 1.4 kb downstream from the stop codon (Fu et al., 2009). We selected plants from two transformation events (17a and 26b) that had the highest transcript levels of *WKS1* (Fu et al., 2009). These transgenic lines were developed by bombardment and have different *WKS1* copy numbers (Fu et al., 2009).

In addition, we developed transgenic wheat lines for five new constructs specifically for this study (Table 1). To determine the effect of *WKS1* alternative splice variants on *Pst* resistance, we generated transgenic Glasgow plants including either the *WKS1.1* or the *WKS1.2* coding regions under the control of the 3.5-kb native promoter (NP:WKS1.1 and NP:WKS1.2). These transgenic lines were developed at the National Institute of Agricultural Botany using the Seed Inoculation Method licensed from Biogemma (Risacher et al., 2009).

Transgenic Bobwhite lines Ubi:TAP-WKS1.1 and NP:WKS1.1-GFP (Table 1) were developed by bombardment using methods described before (Okubara et al., 2002) and summarized briefly in Supplemental Methods 2. The Ubi:TAP-WKS1.1 transgenic wheat plants expressing a fusion protein between the TAP tag (Rohila et al., 2006) and *WKS1* under the regulation of the maize (*Zea mays*) *Ubiquitin* promoter were used for CoIP experiments and to study the effect of the overexpression of *WKS1.1* in the presence and absence of the *tAPX-6B* mutation. The NP:WKS1.1-GFP transgenic wheat plants expressing a fusion protein between *WKS1.1* and GFP under the regulation of the *WKS1* promoter region (3.5 kb) was used to study the subcellular localization of *WKS1.1* in vivo. As a control, we developed additional transgenic wheat plants expressing GFP under the regulation of the same promoter region (NP:GFP). Transgenic lines were evaluated for resistance to race PST-08/21 (Cantu et al., 2013) and PST130 (Cantu et al., 2011).

In Vitro Lipid Assays

To test the ability of the full-length *WKS1.1* and *WKS1.2* and of their respective START domains to bind lipids, we generated four GST fusions and expressed them in wheat germ extracts as described in Supplemental Methods 3. We then tested the ability of these four GST-tagged proteins to bind lipid using two different lipid strips developed by Echelon Biosciences. The first one included 100 pmol of 15 different membrane lipids and the second one included decreasing concentrations of mono-, di-, and triphosphate PIPs (Figure 2). Methods for incubation, washing, and detection are described in Supplemental Methods 3.

Y2H Assays and Library Screening

Pairwise Y2H interactions were performed using the Matchmaker Gold yeast two-hybrid system (Clontech Laboratories) as described before (Li et al., 2011). Gateway-compatible versions of the pGBKT7 (bait) and pGADT7 (prey) vectors were provided by Richard Michelmore (University of California, Davis) and were designated pLAW10 and pLAW11, respectively. Primers used to generate the different yeast constructs are listed in Supplemental Table 2, and the Y2H methods and controls are described in Supplemental Methods 4. To find *WKS1* interactors, we screened a cDNA library generated from RNA extracted from leaves of tetraploid wheat infected with *Puccinia striiformis* race PST113 (Yang et al., 2013) as described in Supplemental Methods 5.

In Vitro Chloroplast Import Assays

Plasmids carrying coding sequences for the full-length *WKS1.1* protein, the *WKS1.1*-GFP fusion, and the *WKS1.1*-START domain were prepared as described in Supplemental Methods 6. Plasmids for DGD1 and Tic40 were as described previously (Froehlich et al., 2001; Tripp et al., 2007). Procedures of chloroplast import assays were described before (Midorikawa and Inoue, 2013).

CoIP

To validate the interaction between *WKS1* and *tAPX* observed in the Y2H experiments, we performed a CoIP experiment, as described in detail in Supplemental Methods 7. Briefly, a total protein extract of leaves from Ubi:TAP-WKS1.1 transgenic plants overexpressing *WKS1.1* was mixed and incubated with IgG Sepharose beads. The TAP-tagged proteins were released by digestion with tobacco etch virus protease and incubated with calmodulin-agarose beads. The eluted proteins were precipitated and loaded onto a 4 to 15% gradient polyacrylamide gel for SDS-PAGE. Proteins were transferred to a nitrocellulose membrane and *tAPX* was detected by protein gel blot using a commercial rabbit anti-*tAPX* antibody (Agriseria; catalog number AS08 368).

Recombinant Protein Purification

The *WKS1.1* kinase domain from *Triticum turgidum* ssp *dicoccoides* and the full-length genes *tAPX* and *PPIP5K1*-like from *Triticum monococcum* accession DV92 were amplified by reverse transcription of leaf mRNA using primers described in Supplemental Table 2. The PCR products were ligated into vectors pET41b (*WKS1.1*-kinase), pET28a (*tAPX*), and pDEST17 (*PPIP5K1*-like), all of which have an N-terminal 6X His tag. Constructs were confirmed by sequencing and were transformed into BL21 (DE3) pLysS-competent cells (Promega). Proteins were purified using the N-terminal 6X His tag with Ni-NTA resin (Pierce Biotechnology) as described in Supplemental Methods 8.

Phosphorylation Assays

To test the ability of the *WKS1*-kinase to phosphorylate *tAPX*, we mixed 2 µg of each recombinant protein in a kinase reaction buffer (100 mM PBS,

pH 7.5, 10 mM MgCl₂, 1 mM ascorbic acid, and 2 mM ATP) for 3 h at room temperature. Methods for the quantitative phosphofluorescence assay (Figure 6A), the in vitro phosphorylation assay separation in SDS-PAGE (Figure 6B), and the in vitro and in planta gel retardation assays (Figures 6C and 6D) are described in detail in Supplemental Methods 9. For the in planta gel retardation assays, we first isolated intact chloroplast from transgenic Bobwhite wheat plants transformed with NP:WKS1 and from nontransgenic Bobwhite lacking WKS1 as control. Proteins were extracted from the intact chloroplasts, and the tAPX protein was detected in protein gel blot using the same commercial rabbit anti-tAPX antibody described above. Controls for the in vitro assays included samples without ATP (Figure 6A) or with the PPIP5K1-like protein, which is not phosphorylated by the WKS1-kinase (Figure 6B).

Recombinant tAPX Activity Assays

tAPX Recombinant Protein

The tAPX recombinant protein was purified as described above and in Supplemental Methods 8. The activity of 2 μg of recombinant tAPX protein was first tested for its ability to decrease H₂O₂ concentration (Supplemental Methods 10). To analyze the effect of WKS1.1 phosphorylation on tAPX activity, we then mixed 2 μg of in vitro-translated WKS1.1 protein with 2 μg of tAPX recombinant protein in a kinase reaction buffer and incubated for 3 h at room temperature. tAPX activity was then determined as described in Supplemental Methods 10.

APX Protein Extracted from Wheat Plants

Wheat-soluble and thylakoid APX activity was compared between transgenic Bobwhite plants transformed with GFP (control) and NP:WKS1 (transgenic lines 26b-15, 26b-6, and 17a-15; Fu et al., 2009). Assays were performed following previously published protocols (Danna et al., 2003) described in detail in Supplemental Methods 10.

Accession Numbers

Sequence data from this article can be found in the GenBank/EMBL data libraries under accession numbers KJ614568 (tAPX), KJ614569 (VAP1), and KJ614570 (PPIP5K1-like).

Supplemental Data

Supplemental Figure 1. Pathogen Growth and Development in Interveinal Regions of Uvitex-Stained Leaves in Three Pairs of Hexaploid Wheat Isogenic Lines with and without *WKS1*.

Supplemental Figure 2. Wheat Plants Transformed with NP:WKS1.1 or NP:WKS1.2 and Inoculated with *Pst* Race PST-08/21.

Supplemental Figure 3. Effect of WKS1.1 Mutations on Homodimer Formation.

Supplemental Figure 4. Y2H Assays between WKS1 Variants and Interacting Proteins tAPX, VAP1-3, and PPIP5K1-Like.

Supplemental Figure 5. Western Blot Confirming that Mutant and Alternative Splice WKS1.2 Proteins Are Not Degraded in Negative Y2H Interactions in Figure 3 and Supplemental Figures 3 and 4.

Supplemental Figure 6. Interaction Between tAPX and Splice Variants WKS1.1 and WKS1.2 by Bimolecular Fluorescence Complementation.

Supplemental Figure 7. Effect of WKS1.1 Fusions with Tags at the N- or C-Terminal Regions on Interactions with Full-Length tAPX in Y2H Assays and on Resistance to *Pst*.

Supplemental Figure 8. Controls for the in Vitro Chloroplast Import Assays.

Supplemental Figure 9. Effect of Different Ions and pH on tAPX Activity in Vitro.

Supplemental Figure 10. Validation of the Interaction between VAP1-3 and WKS1.1 by Bimolecular Fluorescence Complementation in *N. benthamiana* Protoplasts.

Supplemental Table 1. Average Resistance of Plants Transformed with NP:WKS1.1 and NP:WKS1.2 and Inoculated with *Pst* Race PST-08/21.

Supplemental Table 2. Primers Used in This Study.

Supplemental Table 3. WKS1 Protein Interactors Detected in Y2H Screen and Their Y2H Interactions with Alternative Splice Variants WKS1.1 and WKS1.2 and Mutants (*wks1a-e*).

Supplemental Methods 1. Time Course of *Pst* Infection.

Supplemental Methods 2. Transgenic Lines.

Supplemental Methods 3. In Vitro Lipid Binding Assays.

Supplemental Methods 4. Yeast Two-Hybrid Assays.

Supplemental Methods 5. Wheat cDNA Y2H Library Screening and Validation.

Supplemental Methods 6. In Vitro Chloroplast Localization.

Supplemental Methods 7. Coimmunoprecipitation.

Supplemental Methods 8. Recombinant WKS1-Kinase, tAPX, and PPIP5K1-Like Protein Purification.

Supplemental Methods 9. Phosphorylation Assays.

Supplemental Methods 10. tAPX Activity Assays.

ACKNOWLEDGMENTS

This project was supported by National Research Initiative Competitive Grant 2011-68002-30029 (Triticeae-CAP) from the USDA National Institute of Food and Agriculture, by US-Israel BARD Grants US-4323-10C and IS-4628-13, by Division of Chemical Sciences, Geosciences, and Biosciences, Office of Basic Energy Sciences of the U.S. Department of Energy Grant DE-FG02-08ER15963, by the Major International Joint Research Project (31110103917) from the National Natural Science Foundation of China, and by the SCPRID Program (BB/J012017/1) from the Biotechnology and Biological Science Research Council. J.D. acknowledges the financial support of the Howard Hughes Medical Institute and Gordon & Betty Moore Foundation. J.-Y.G. is supported by The Program for Professor of Special Appointment (Eastern Scholar) at Shanghai Institutions of Higher Learning (SHH1322012) and the National Natural Science Foundation of China (31470386). C.U. and E.W. acknowledge financial support from the National Institute of Agricultural Botany Trust and thank M. Craze and S. Bowden for transformation of wheat variety Glasgow as well as R. LeFevre and R. Howells for technical assistance. A.D.-A. is supported by a Marie Curie fellowship. The USDA is an equal opportunity provider and employer. Mention of a specific product name by the USDA does not constitute an endorsement and does not imply a recommendation over other suitable products.

AUTHOR CONTRIBUTIONS

J.D., C.U., D.F., T.F., and J.-Y.G. designed the research. J.-Y.G. performed senescence and APX experiments and coordinated the

experiments. M.M. and L.E. performed the *Pst* time course. E.W., A.D.-A., and C.U. developed and characterized the NP:WKS1.1 and NP:WKS1.2 transgenic plants. A.B. developed the Ubi:TAP-WKS1.1 and NP:WKS1.1-GFP transgenic plants. D.C. characterized the cellular localization. X.W., K.W., K.L., and D.F. performed protein-protein interaction assays. H.L. and X.W. performed the bimolecular fluorescence complementation assays, and J.S. performed the lipid binding assays. T.M. conducted protein import assay using isolated chloroplasts, and T.M. and K.I. analyzed the data. J.-Y.G. wrote the first version of the article. All authors contributed to the analysis of the data and to the review of the article. J.D. revised the article, integrated the corrections, and produced the final version.

Received November 24, 2014; revised April 21, 2015; accepted April 26, 2015; published May 19, 2015.

REFERENCES

- Alpy, F., and Tomasetto, C. (2014). START ships lipids across interorganelle space. *Biochimie* **96**: 85–95.
- Andersson, M.X., Kourtchenko, O., Dangl, J.L., Mackey, D., and Ellerström, M. (2006). Phospholipase-dependent signalling during the AvrRpm1- and AvrRpt2-induced disease resistance responses in *Arabidopsis thaliana*. *Plant J.* **47**: 947–959.
- Armbruster, U., Hertle, A., Makarenko, E., Zühlke, J., Pribil, M., Dietzmann, A., Schliebner, I., Aseeva, E., Fenino, E., Scharfenberg, M., Voigt, C., and Leister, D. (2009). Chloroplast proteins without cleavable transit peptides: rare exceptions or a major constituent of the chloroplast proteome? *Mol. Plant* **2**: 1325–1335.
- Belhaj, K., Lin, B., and Mauch, F. (2009). The chloroplast protein RPH1 plays a role in the immune response of *Arabidopsis* to *Phytophthora brassicae*. *Plant J.* **58**: 287–298.
- Bradley, D.J., Kjellbom, P., and Lamb, C.J. (1992). Elicitor- and wound-induced oxidative cross-linking of a proline-rich plant cell wall protein: a novel, rapid defense response. *Cell* **70**: 21–30.
- Brevis, J.C., Chicaiza, O., Khan, I.A., Jackson, L., Morris, C.F., and Dubcovsky, J. (2008). Agronomic and quality evaluation of common wheat near-isogenic lines carrying the leaf rust resistance gene *Lr47*. *Crop Sci.* **48**: 1441–1451.
- Cantu, D., Govindarajulu, M., Kozik, A., Wang, M., Chen, X., Kojima, K.K., Jurka, J., Michelmore, R.W., and Dubcovsky, J. (2011). Next generation sequencing provides rapid access to the genome of *Puccinia striiformis* f. sp. *tritici*, the causal agent of wheat stripe rust. *PLoS ONE* **6**: e24230.
- Cantu, D., Segovia, V., MacLean, D., Bayles, R., Chen, X., Kamoun, S., Dubcovsky, J., Saunders, D.G.O., and Uauy, C. (2013). Genome analyses of the wheat yellow (stripe) rust pathogen *Puccinia striiformis* f. sp. *tritici* reveal polymorphic and haustorial expressed secreted proteins as candidate effectors. *BMC Genomics* **14**: 270.
- Caplan, J.L., Mamillapalli, P., Burch-Smith, T.M., Czymbek, K., and Dinesh-Kumar, S.P. (2008). Chloroplastic protein NRIP1 mediates innate immune receptor recognition of a viral effector. *Cell* **132**: 449–462.
- Caverzan, A., Passaia, G., Rosa, S.B., Ribeiro, C.W., Lazzarotto, F., and Margis-Pinheiro, M. (2012). Plant responses to stresses: Role of ascorbate peroxidase in the antioxidant protection. *Genet. Mol. Biol.* **35** (suppl.): 1011–1019.
- Clark, B.J. (2012). The mammalian START domain protein family in lipid transport in health and disease. *J. Endocrinol.* **212**: 257–275.
- Cline, K., Werner-Washburne, M., Andrews, J., and Keegstra, K. (1984). Thermolysin is a suitable protease for probing the surface of intact pea chloroplasts. *Plant Physiol.* **75**: 675–678.
- Coll, N.S., Eppe, P., and Dangl, J.L. (2011). Programmed cell death in the plant immune system. *Cell Death Differ.* **18**: 1247–1256.
- Danna, C.H., Bartoli, C.G., Sacco, F., Ingala, L.R., Santa-Maria, G.E., Guiamet, J.J., and Ugalde, R.A. (2003). Thylakoid-bound ascorbate peroxidase mutant exhibits impaired electron transport and photosynthetic activity. *Plant Physiol.* **132**: 2116–2125.
- de Jong, C.F., Laxalt, A.M., Bargmann, B.O.R., de Wit, P.J.G.M., Joosten, M.H.A.J., and Munnik, T. (2004). Phosphatidic acid accumulation is an early response in the Cf-4/Avr4 interaction. *Plant J.* **39**: 1–12.
- Feng, H., Wang, X., Zhang, Q., Fu, Y., Feng, C., Wang, B., Huang, L., and Kang, Z. (2014). Monodehydroascorbate reductase gene, regulated by the wheat PN-2013 miRNA, contributes to adult wheat plant resistance to stripe rust through ROS metabolism. *Biochim. Biophys. Acta* **1839**: 1–12.
- Froehlich, J.E., Benning, C., and Dörmann, P. (2001). The digalactosyldiacylglycerol (DGDG) synthase DGD1 is inserted into the outer envelope membrane of chloroplasts in a manner independent of the general import pathway and does not depend on direct interaction with monogalactosyldiacylglycerol synthase for DGDG biosynthesis. *J. Biol. Chem.* **276**: 31806–31812.
- Fu, D., Uauy, C., Distelfeld, A., Blechl, A., Epstein, L., Chen, X., Sela, H., Fahima, T., and Dubcovsky, J. (2009). A kinase-START gene confers temperature-dependent resistance to wheat stripe rust. *Science* **323**: 1357–1360.
- Greenberg, J.T. (1996). Programmed cell death: a way of life for plants. *Proc. Natl. Acad. Sci. USA* **93**: 12094–12097.
- Hovmöller, M.S., Walter, S., and Justesen, A.F. (2010). Escalating threat of wheat rusts. *Science* **329**: 369.
- Hung, C.Y., Aspesi, P., Jr., Hunter, M.R., Lomax, A.W., and Perera, I.Y. (2014). Phosphoinositide-signaling is one component of a robust plant defense response. *Front. Plant Sci.* **5**: 267.
- Krattinger, S.G., Lagudah, E.S., Spielmeier, W., Singh, R.P., Huerta-Espino, J., McFadden, H., Bossolini, E., Selter, L.L., and Keller, B. (2009). A putative ABC transporter confers durable resistance to multiple fungal pathogens in wheat. *Science* **323**: 1360–1363.
- Levine, A., Tenhaken, R., Dixon, R., and Lamb, C. (1994). H₂O₂ from the oxidative burst orchestrates the plant hypersensitive disease resistance response. *Cell* **79**: 583–593.
- Li, C., Distelfeld, A., Comis, A., and Dubcovsky, J. (2011). Wheat flowering repressor VRN2 and promoter CO2 compete for interactions with NUCLEAR FACTOR-Y complexes. *Plant J.* **67**: 763–773.
- Loewen, C.J.R., and Levine, T.P. (2005). A highly conserved binding site in vesicle-associated membrane protein-associated protein (VAP) for the FFAT motif of lipid-binding proteins. *J. Biol. Chem.* **280**: 14097–14104.
- Lowe, I., Cantu, D., and Dubcovsky, J. (2011). Durable resistance to the wheat rusts: integrating systems biology and traditional phenotype-based research methods to guide the deployment of resistance genes. *Euphytica* **179**: 69–79.
- Maccaferri, M., Zhang, J., Bulli, P., Abate, Z., Chao, S., Cantu, D., Bossolini, E., Chen, X., Pumphrey, M., and Dubcovsky, J. (2015). A genome-wide association study of resistance to stripe rust (*Puccinia striiformis* f. sp. *tritici*) in a worldwide collection of hexaploid spring wheat (*Triticum aestivum* L.). G3 (Bethesda) **5**: 449–465.
- Maruta, T., Tanouchi, A., Tamoi, M., Yabuta, Y., Yoshimura, K., Ishikawa, T., and Shigeoka, S. (2010). Arabidopsis chloroplastic ascorbate peroxidase isoenzymes play a dual role in photoprotection and gene regulation under photooxidative stress. *Plant Cell Physiol.* **51**: 190–200.
- McIntosh, R.A., Yamazaki, Y., Dubcovsky, J., Rogers, W.J., Morris, C.F., Appels, R., and Xia, X.C. (2013). Catalogue of Gene Symbols for Wheat. (<http://wheat.pw.usda.gov/GG2/Triticum/wgc/2013/GeneCatalogueIntroduction.pdf>).

- Michelmore, R.W., Christopoulou, M., and Caldwell, K.S.** (2013). Impacts of resistance gene genetics, function, and evolution on a durable future. *Annu. Rev. Phytopathol.* **51**: 291–319.
- Midorikawa, T., and Inoue, K.** (2013). Multiple fates of non-mature luminal proteins in thylakoids. *Plant J.* **76**: 73–86.
- Milus, E.A., Kristensen, K., and Hovmøller, M.S.** (2009). Evidence for increased aggressiveness in a recent widespread strain of *Puccinia striiformis* f. sp. *tritici* causing stripe rust of wheat. *Phytopathology* **99**: 89–94.
- Munnik, T., and Vermeer, J.E.M.** (2010). Osmotic stress-induced phosphoinositide and inositol phosphate signalling in plants. *Plant Cell Environ.* **33**: 655–669.
- Nakagawa, T., Kurose, T., Hino, T., Tanaka, K., Kawamukai, M., Niwa, Y., Toyooka, K., Matsuoka, K., Jinbo, T., and Kimura, T.** (2007). Development of series of gateway binary vectors, pGWBs, for realizing efficient construction of fusion genes for plant transformation. *J. Biosci. Bioeng.* **104**: 34–41.
- Okubara, P.A., Blechl, A.E., McCormick, S.P., Alexander, N.J., Dill-Macky, R., and Hohn, T.M.** (2002). Engineering deoxynivalenol metabolism in wheat through the expression of a fungal trichothecene acetyltransferase gene. *Theor. Appl. Genet.* **106**: 74–83.
- Park, J., Gu, Y., Lee, Y., Yang, Z., and Lee, Y.** (2004). Phosphatidic acid induces leaf cell death in Arabidopsis by activating the Rho-related small G protein GTPase-mediated pathway of reactive oxygen species generation. *Plant Physiol.* **134**: 129–136.
- Pavet, V., Olmos, E., Kiddle, G., Mowla, S., Kumar, S., Antoniw, J., Alvarez, M.E., and Foyer, C.H.** (2005). Ascorbic acid deficiency activates cell death and disease resistance responses in Arabidopsis. *Plant Physiol.* **139**: 1291–1303.
- Radhamony, R.N., and Theg, S.M.** (2006). Evidence for an ER to Golgi to chloroplast protein transport pathway. *Trends Cell Biol.* **16**: 385–387.
- Raho, N., Ramirez, L., Lanteri, M.L., Gonorazky, G., Lamattina, L., ten Have, A., and Laxalt, A.M.** (2011). Phosphatidic acid production in chitosan-elicited tomato cells, via both phospholipase D and phospholipase C/diacylglycerol kinase, requires nitric oxide. *J. Plant Physiol.* **168**: 534–539.
- Risacher, T., Craze, M., Bowden, S., Paul, W., and Barsby, T.** (2009). Highly efficient *Agrobacterium*-mediated transformation of wheat via *in planta* inoculation. In *Methods in Molecular Biology: Transgenic Wheat, Barley and Oats*, H.D. Jones and P.R. Shewry, eds (New York: Humana Press), pp. 115–124.
- Rohila, J.S., et al.** (2006). Protein-protein interactions of tandem affinity purification-tagged protein kinases in rice. *Plant J.* **46**: 1–13.
- Sacco, F., Suarez, E.Y., and Naranjo, T.** (1998). Mapping of the leaf rust resistance gene *Lr3* on chromosome 6B of Sinvalocho MA wheat. *Genome* **41**: 686–690.
- Schrack, K., Nguyen, D., Karlowski, W.M., and Mayer, K.F.X.** (2004). START lipid/sterol-binding domains are amplified in plants and are predominantly associated with homeodomain transcription factors. *Genome Biol.* **5**: R41.
- Schrack, K., Bruno, M., Khosla, A., Cox, P.N., Marlatt, S.A., Roque, R.A., Nguyen, H.C., He, C., Snyder, M.P., Singh, D., and Yadav, G.** (2014). Shared functions of plant and mammalian STAR-related lipid transfer (START) domains in modulating transcription factor activity. *BMC Biol.* **12**: 70.
- Shi, L.X., and Theg, S.M.** (2013). The chloroplast protein import system: From algae to trees. *Biochim. Biophys. Acta* **1833**: 314–331.
- Shigeoka, S., Ishikawa, T., Tamoi, M., Miyagawa, Y., Takeda, T., Yabuta, Y., and Yoshimura, K.** (2002). Regulation and function of ascorbate peroxidase isoenzymes. *J. Exp. Bot.* **53**: 1305–1319.
- Spoel, S.H., and Dong, X.** (2012). How do plants achieve immunity? Defence without specialized immune cells. *Nat. Rev. Immunol.* **12**: 89–100.
- Stahl, T., Glockmann, C., Soll, J., and Heins, L.** (1999). Tic40, a new “old” subunit of the chloroplast protein import translocon. *J. Biol. Chem.* **274**: 37467–37472.
- Staiger, D., and Brown, J.W.S.** (2013). Alternative splicing at the intersection of biological timing, development, and stress responses. *Plant Cell* **25**: 3640–3656.
- Syed, N.H., Kalyna, M., Marquez, Y., Barta, A., and Brown, J.W.S.** (2012). Alternative splicing in plants—coming of age. *Trends Plant Sci.* **17**: 616–623.
- Tang, D., Ade, J., Frye, C.A., and Innes, R.W.** (2005). Regulation of plant defense responses in Arabidopsis by EDR2, a PH and START domain-containing protein. *Plant J.* **44**: 245–257.
- Testerink, C., and Munnik, T.** (2011). Molecular, cellular, and physiological responses to phosphatidic acid formation in plants. *J. Exp. Bot.* **62**: 2349–2361.
- Torres, M.A.** (2010). ROS in biotic interactions. *Physiol. Plant.* **138**: 414–429.
- Tripp, J., Inoue, K., Keegstra, K., and Froehlich, J.E.** (2007). A novel serine/proline-rich domain in combination with a transmembrane domain is required for the insertion of AtTic40 into the inner envelope membrane of chloroplasts. *Plant J.* **52**: 824–838.
- Vorwerk, S., Schiff, C., Santamaria, M., Koh, S., Nishimura, M., Vogel, J., Somerville, C., and Somerville, S.** (2007). *EDR2* negatively regulates salicylic acid-based defenses and cell death during powdery mildew infections of *Arabidopsis thaliana*. *BMC Plant Biol.* **7**: 35.
- Wang, C.F., Huang, L.L., Buchenauer, H., Han, Q.M., Zhang, H.C., and Kang, Z.S.** (2007). Histochemical studies on the accumulation of reactive oxygen species (O_2^- and H_2O_2) in the incompatible and compatible interaction of wheat - *Puccinia striiformis* f. sp. *tritici*. *Physiol. Mol. Plant Pathol.* **71**: 230–239.
- Yang, B., Ruan, R., Cantu, D., Wang, X., Ji, W., Ronald, P.C., and Dubcovsky, J.** (2013). A comparative approach expands the protein-protein interaction node of the immune receptor *XA21* in wheat and rice. *Genome* **56**: 315–326.